

# Finite curvature continuous polar patchworks

Kęstutis Karčiauskas<sup>0</sup>, Jörg Peters<sup>1</sup>

<sup>0</sup>Vilnius University, <sup>1</sup>University of Florida

**Abstract.** We present an algorithm for completing a  $C^2$  surface of up to degree bi-6 by capping an  $n$ -sided hole with polar layout. The cap consists of  $n$  tensor-product patches, each of degree 6 in the periodic and degree 5 in the radial direction. To match the polar layout, one edge of these patches is collapsed. We explore and compare with alternative constructions, based on more pieces or using total-degree, triangular patches.

## 1 Introduction

Vertices of high valence occur in control nets of surfaces of revolution and similar objects and as higher-order saddle points; see Figure 1. Representing the neighborhood of such a high-valent vertex in *polar layout*, i.e. surrounding the point by one layer of triangles while the next layer of facets consists of quadrilaterals with always four joining at a vertex, is a natural and compatible addition to the established tensor-product layout of patches (see e.g. [1]). Polar layout can be used to define subdivision surfaces (see Section 1.1), but engineers may well prefer finite constructions, in the sense that the final output surface consists of a finite number of polynomial or rational patches. Here, we therefore present *finite polar curvature continuous patchworks* that fill an  $n$ -sided hole in an existing tensor-product spline complex.

Away from the central *polar vertex*, the net as in Figure 1 can be interpreted as the control net of a  $C^2$  spline; for example a bi-3 spline. However, assuming that the tensor-border is obtained from a piecewise bi-3 layer of patches generated from a polar mesh is in general too restrictive for high-quality modeling. More generally, we consider the following input: position, first and second derivative along a closed curve of degree up to 6. We call such input a *tensor-border* of degree  $p$  if curve and derivatives are

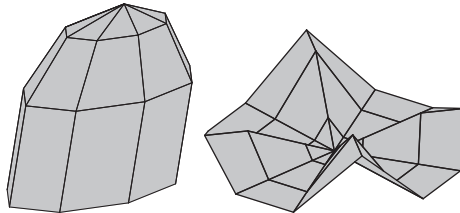


**Fig. 1. Polar layout:** (left) elliptic 8-sided dome; (right) 12-sided higher-order saddle.

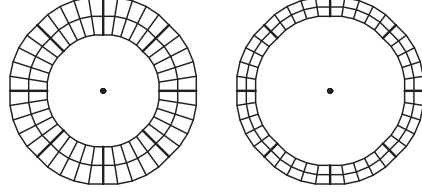


**Fig. 2. Tensor-border input:** (left) A degree 3 polar tensor-border derived from a polar control net, raised to degree 5; the central point is set to the limit point of bi-3 polar subdivision [2]. (right) A degree 5 tensor-border not generated from a polar control net; the derivatives may be scaled before applying Algorithm I. The central point is user-set.

of degree at most  $p$ . Figure 2 shows two tensor-borders represented by coefficients in tensor-product BB-form (Bernstein-Bézier form; see e.g. [3]).

In the following, we discuss and compare several possible approaches to constructing a cap that matches a given tensor-border. Section 2 contains the main construction: Algorithm I generates one patch for each of the  $n$  sectors of the polar layout. Each patch is of *degree 6-5*, degree 6 in the periodic direction (circulating around the pole) and degree 5 in the radial direction (emanating from the pole); one periodic edge is collapsed to form the pole. Most CAD packages do not mind tensor-product patches with one collapsed edge. However, it raises the question, whether we can achieve the same good quality with similar polynomial degree and without collapse, using, say, ‘triangular’ patches. Section 3.1 shows that this is indeed possible (Algorithm II) and also presents a non-collapsed construction using multiple tensor-product pieces (Algorithm III). Section 3.2 shows that we can alternatively reduce the degree to bi-5 using a collapsed-edge representation. The resulting curvature continuous patchworks show good curvature distribution but the construction comes at the cost of (considerably) more patches per sector (Algorithm IV). The discussion section points out that non-uniformly spaced parameterizations are easy to realize within the same framework.

### 1.1 Related Literature

A simple mesh-based algorithm generating  $C^1$  limit surfaces of degree bi-3 with polar layout was introduced in [2]. The bi-3 construction can be joined with Catmull-Clark subdivision [4] in a natural fashion [1]. *Guided*  $C^2$  subdivision, both for the polar and for the all-quadrilateral layout of Catmull-Clark appeared in [5]. [1] showed a construction with a fixed, finite number of patches that is functionally equivalent to the polar subdivision scheme defined in [2]. Similarly, a number of constructions have recently been developed to improve on Catmull-Clark surfaces in a finite setting [6–10]. Finite guided  $C^2$  surface constructions via  $G^2$  patchworks with the layout of a Catmull-Clark input mesh, using patches of degree bi-6 or even only bi-5 have been announced. Degenerate (triangular) Bézier patches joining with continuous curvature were analyzed in [11].

## 2 $C^2$ polar cap construction using one patch of degree 6-5 per sector

Figure 3 illustrates the structure of each patch of degree 6-5 and Figure 4 shows a constructed surface. The construction has four ingredients explained in detail in Section

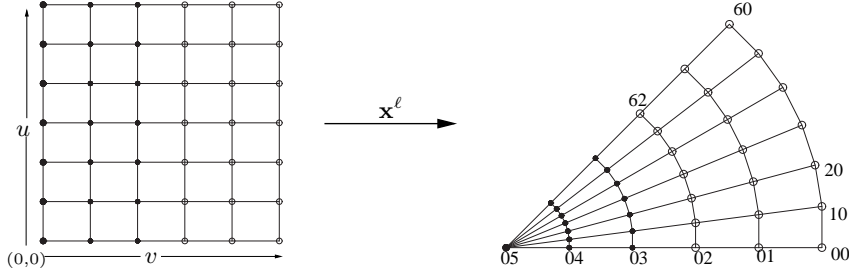


**Fig. 3.** A 6-5 patch  $\mathbf{x}^\ell : [0..1]^2 \rightarrow \mathbb{R}^3$  of degree 6 in the periodic and degree 5 in the radial direction. (left) Domain, (right) patch with one edge collapsed: for  $i = 0, \dots, 6$ ,  $\mathbf{x}_{i5}$  is the pole. The BB-coefficients displayed as circles are defined by the tensor-border. The BB-coefficients displayed as black disks are defined by a quadratic expansion at the central point.

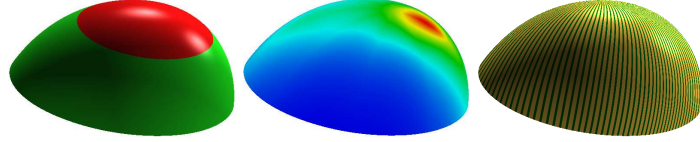


**Fig. 4.** A 6-5 convex completion of a surface. (left) Bi-3 input ring (green, defining the tensor-border) and 6-5 cap (red); (middle) Gaussian curvature shading; (right) highlight shading.

2.1:

1. a guide surface cap  $\mathbf{q} : \Omega \subsetneq \mathbb{R}^2 \mapsto \mathbb{R}^3$  consisting of  $n$  triangular patches of total degree 2 (gray region in Figure 5 middle) ;
2. a polar concentric tessellation map (*ct-map*),  $\rho : [0..1]^2 \times \{1, \dots, n\} \rightarrow \mathbb{R}^2$  (Figure 5 left) ;
3. the operator  $H_{n,p}$  that defines a surface ring or cap of  $n$  patches of periodic degree  $p$  and radial degree 5 by (Hermite-)interpolating position, first and second derivative at its two periodic edges ;
4. the functional

$$\mathcal{F} : C^m([0..1]^2) \ni f \rightarrow \mathcal{F}_m(f) := \int_{\square} \sum_{i+j=m; i,j \geq 0} \binom{m}{i,j} (\partial_{u^i v^j}^m f)^2 \quad (1)$$

that acts on sufficiently smooth functions  $f$  defined over the unit square  $[0..1]^2$ .

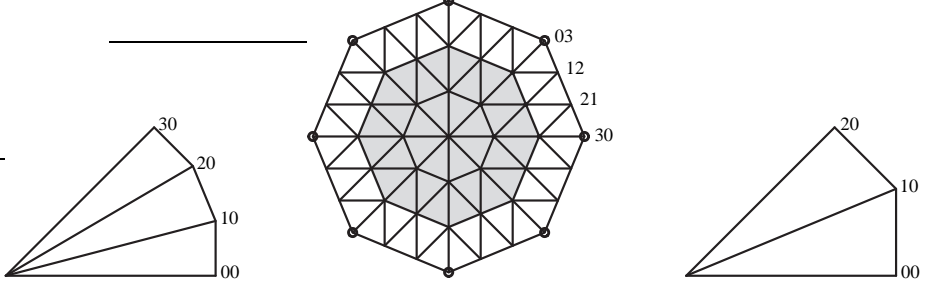


**Fig. 5. Polar reparameterizations (ct-maps) and guide surfaces.** One sector (*left*) of the  $C^2$  bi-31 ct-map  $\rho$ , (*right*) of the  $C^2$  bi-21 ct-map  $\rho_2$ . (*middle*) BB control net  $p_{jk}^l$  of a guide patch  $q$  of degree 2 (gray area, 2-link) or  $c$  of degree 3. (Note the different indexing conventions for (collapsed) tensor-product and total degree patches.)

## 2.1 The ingredients

1. The piecewise quadratic guide  $q$  consisting of  $n$  triangular, total-degree 2 polynomial pieces forms a  $C^2$  map if all pieces define the same quadratic. In other words, its Bernstein-Bézier (BB)-coefficients  $p_{00}^\ell, p_{10}^\ell, p_{01}^\ell, p_{20}^\ell, p_{11}^\ell, p_{02}^\ell$  (gray region in Figure 5 *middle*) are defined by one piece, say  $\ell = 0$ .

2. The polar concentric tessellation map (*ct-map*) (Figure 5 *left*),

$$\rho : [0..1]^2 \times \{1, \dots, n\} \rightarrow \mathbb{R}^2$$

that reparameterizes the domain is defined as follows. Its  $\ell$ th sector is defined by a template map  $r : [0..1]^2 \rightarrow \mathbb{R}^2$  rotated about the origin by  $\ell \frac{2\pi}{n}$ . The template map is of degree bi-31, i.e. of degree 3 in the periodic  $u$ -direction and degree 1 in the radial  $v$ -direction (see Figure 5 *left*). Its BB-coefficients are  $r_{i1} := [\begin{smallmatrix} 0 \\ 1 \end{smallmatrix}]$ ,  $i = 0, 1, 2, 3$ ,

$$r_{00} := [\begin{smallmatrix} 1 \\ 0 \end{smallmatrix}], r_{10} := \left[ \begin{array}{c} 1 \\ \frac{\sin \alpha}{2 + \cos \alpha} \end{array} \right], r_{20} := R_\alpha r_{10}, r_{30} := R_\alpha r_{00} = [\begin{smallmatrix} \cos \alpha \\ \sin \alpha \end{smallmatrix}], \alpha := \frac{2\pi}{n},$$

where  $R_\alpha$  is the reflection across the line through the origin and  $[\cos \frac{\alpha}{2}, \sin \frac{\alpha}{2}]$ . By construction, the polynomial pieces of  $\rho$  join formally  $C^2$  across the sector boundaries.

3. The operator  $H_{n,p}(b_0, b_1)$  defines a  $C^2$  surface ring or cap  $x \in C^2([0..1]^2 \times \{1, \dots, n\})$  consisting of  $n$  polynomial patches of periodic degree  $p$  and radial degree 5 uniquely determined by (Hermite-)interpolating position, first and second derivative (the tensor-borders  $b_k$  of degree  $p$ ) at its two periodic edges corresponding to  $v = 0$  and  $v = 1$ , respectively. We denote by  $J(f, v)$ , a tensor-border read off from a patch  $f \in C^2([0..1]^2 \times \{1, \dots, n\})$  at its radial parameter  $v$ .

Below we will build a patch  $x$  of degree 6-5 as shown in Figure 3. Three layers of BB-coefficients marked as black disks are defined by  $b_0$  and three layers marked by circles are defined by  $b_1$ .

### Algorithm I: $C^2$ cap construction of degree 6-5

*Input.* The tensor-border  $b$  of the hole in a  $C^2$  patch complex. The position of the pole

(see Figure 2).

*Output.* The  $n$  pieces  $\mathbf{x}^\ell$  of the output surface cap  $\mathbf{x} : [0..1]^2 \times \{1, \dots, n\} \rightarrow \mathbb{R}^3$  (see Figure 3, right) of degree 6-5, i.e. of degree 6 in the periodic direction with one periodic edge collapsed to form the pole and degree 5 in the radial direction.

*Algorithm:* Set the pole, for example to the limit of bi-3 polar subdivision [2] (cf. Figure 2). Form  $\mathbf{q} \circ \rho$  (with five BB-coefficients  $\mathbf{q}_k$ ,  $k = 1, \dots, 5$  still undetermined) and solve the linear  $5 \times 5$  system

$$\min_{\mathbf{q}_k} \mathcal{F}_3 H_{n,6}(J(\mathbf{q} \circ \rho, 0); \mathbf{b}), \quad (2)$$

i.e. minimize the sum of the functionals applied to each of the  $n$  patches in terms of the unknown five BB-coefficients.

**Theorem 1.** *The 6-5 construction yields a  $C^2$  surface.*

**Proof** Since  $\mathbf{b}$  extends the  $C^2$  patch complex and  $\mathbf{q} \circ \rho$  is parametrically  $C^2$  except possibly where it is singular, we need only show that the surface is also  $C^2$  at the central point. For this we construct an auxiliary subdivision algorithm of type (1/2,1/4,0) [12, Ch 7] as follows. Denote the univariate degree 3 boundary of the template of  $\rho$  by  $r_\circ \in \mathbb{R}^2$  and the  $\frac{2\pi}{n}$  rotation matrix by  $R$ . With  $v = 0$  corresponding to the collapsed edge, and recalling that the Taylor expansion of any 6-5 patch  $\mathbf{x}^\ell$  generated by Algorithm I at  $(u, 0)$  is up to second order determined by  $\mathbf{q} \circ \rho^\ell = \mathbf{q}(vR^\ell r_\circ(u))$ , we can write

$$\mathbf{x}^\ell(u, v) := \mathbf{q}_0 + v[\mathbf{q}_1, \mathbf{q}_2](R^\ell r_\circ(u)) + v^2(R^\ell r_\circ(u))^T \begin{bmatrix} \mathbf{q}_3 & \mathbf{q}_4 \\ \mathbf{q}_4 & \mathbf{q}_5 \end{bmatrix} (R^\ell r_\circ(u)) + o(v^2).$$

Repeated subdivision (by De Casteljau's algorithm) of this representation in the radial direction, at  $v = 1/2^m$  yields a sequence of  $C^2$  polar 6-5 rings converging to the pole with  $v$ -monomial eigenfunctions and eigencoefficients  $\mathbf{q}_k$ . In particular, for  $j = 1$  there are two (rather than  $n$ ) distinct  $C^2$  eigenfunctions  $e_{10}$  and  $e_{11}$  and for  $j = 2$  there are three,  $e_{20}$ ,  $e_{21}$  and  $e_{22}$  such that  $e_{20}, e_{21}, e_{22} \in \text{span}\{e_{10}^2, e_{10}e_{11}, e_{11}^2\}$ . [12, Thm 7.16] then applies and completes the proof.  $\|\|$

A similar proof, for  $C^1$  continuity, appeared in [1].

**Theorem 2 (periodic degree estimation).** *For generic tensor-border data, a parametrically  $C^2$  polar cap assembled from  $n$  patches by a symmetric (invariant under index shift and flip) algorithm must have periodic degree at least 6.*

**Proof** By [12, Thm 7.16], a (polar) subdivision algorithm of type (1/2,1/4,0) must be of periodic degree at least twice the periodic degree of its  $C^2$  (polar) characteristic ring. Since the periodic degree is at least three the algorithm must generically generate surfaces of periodic degree 6. The proof of Theorem 1 shows that any symmetric parametrically  $C^2$  polar cap of periodic degree  $m$  induces a polar  $C^2$  subdivision algorithm of type (1/2,1/4,0) that is of periodic degree  $m$ . Therefore  $m \geq 6$  must hold.  $\|\|$

We conclude with examples where the tensor border has not been derived from a control mesh. In Figure 6, the input tensor-border (green in left) is defined by nine  $C^2$ -connected generalized cylinders of periodic degree 5. In the airplane wing tip data of Figure 7, the challenge is to slowly blend the sharp edge into a rounded cap. To

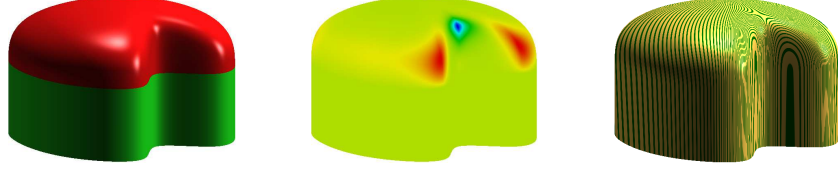


**Fig. 6.** A 6-5 construction for input not derived from a polar control net. (*left*) Input and cap; (*middle*) Gaussian shading; (*right*) highlights.

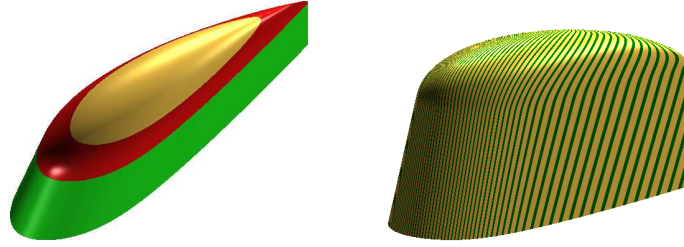


**Fig. 7. Wing tips** feathering out a sharp edge. (*left*) Input data (green) with a sharp edge, transition ring (red) mediating from the sharp edge to the smooth cap and  $C^2$  6-5 cap (gold); (*right*) highlight rendering thereof.

obtain the transition, Algorithm I is applied with a crease in the tensor-border along a sector partitioning curve. The patches are then subdivided in the radial direction and the resulting transition surface ring is adjusted to have three  $C^2$ -connected innermost layers of BB-coefficients. Then Algorithm I is applied a second time with the transition ring now providing the tensor-border  $\mathbf{b}$  (*red* in Figure 7 *left*).

### 3 Alternative constructions

Below, we explore constructions without edge collapse (Algorithm II and III) and with edge collapse (Algorithm IV) where we trade lower degree for (many) more patches compared to the surface construction of Algorithm I. While these three alternative constructions yield equally good shape and continuity as Algorithm I, we think that the trade-off will only rarely be justified. However, we present these alternatives to complete the picture but move fast on the details.

#### 3.1 $C^2$ capping without collapsed edge

In this section, we present two  $C^2$  surface constructions without edge collapse. We leverage the 6-5 cap  $\mathbf{x} : [0..1]^2 \times \{1, \dots, n\} \rightarrow \mathbb{R}^3$  constructed by Algorithm I to provide data from which to determine a  $C^2$  guide surface  $\mathbf{p} : \Omega \subsetneq \mathbb{R}^2 \mapsto \mathbb{R}^3$  (see below and Figure 5 *middle*) of degree 3, that is then composed with a reparametrization  $\tau : [0..1]^2 \times \{1, \dots, n\} \rightarrow \Omega$ . Specifically, we

- (i) extract data from  $\mathbf{x}$  to be matched,

- (ii) extract the same data from  $\mathbf{p} \circ \tau$  (in terms of free coefficients of  $\mathbf{p}$ ), and
- (iii) set the free coefficients by minimizing the difference of the data in (i) and (ii). Then the final surface is essentially (ii) with the coefficients set by (iii).

**Ingredients** Analogous to Section 2.1, we define

**1'.** a guide  $\mathbf{c}$  consisting of  $n$  polynomial pieces of total degree 3. The conditions on its BB-coefficients  $\mathbf{p}_{jk}^\ell$  to be part of a piecewise  $C^2$  map [3] require, (a) the 2-link of the central point  $\mathbf{p}_{00}^\ell$  define the same quadratic polynomial (in possibly degree-raised BB-form) for all  $\ell$  (see the earlier construction of  $\mathbf{q}$ ), and (b) The coefficients  $\mathbf{p}_{30}^\ell$  can be chosen freely; then, for  $n \geq 7$  (which will hold since we trisect each sector),

$$\begin{aligned}\mathbf{p}_{21}^j &:= \frac{1}{n} \sum_{\ell=0}^{n-1} \sum_{k=0}^{n-1} \frac{R_\ell \cos((j-\ell)k\alpha)}{2\mathbf{c} + \cos(k\alpha)}, \\ R_\ell &:= 2\mathbf{c}^2 \mathbf{p}_{30}^\ell + \mathbf{c} \mathbf{p}_{03}^\ell + 4\mathbf{c}(1-\mathbf{c}) \mathbf{p}_{20}^\ell \\ &\quad - 2(1-\mathbf{c}) \mathbf{p}_{11}^\ell + (1-\mathbf{c}) \mathbf{p}_{02}^\ell + 2(1-\mathbf{c})^2 \mathbf{p}_{10}^\ell, \\ \mathbf{c} &:= \cos \alpha, \quad \alpha := 2\pi/n,\end{aligned}\tag{3}$$

and setting subsequently the coefficients  $\mathbf{p}_{12}^\ell$  to satisfy  $C^1$  constraints across the sector lines, makes  $\mathbf{p}$  a  $C^2$  function.

**2'.** Analogous to the definition of  $\rho$  in the previous section, we define the piecewise quadratic  $G^2$  ct-map  $\rho_2$  by rotations of a bi-21 template  $r$  with BB-coefficients

$$r_{i1} := \begin{bmatrix} 0 \\ 0 \end{bmatrix}, \quad r_{00} := \begin{bmatrix} 1 \\ 0 \end{bmatrix}, \quad r_{10} := \begin{bmatrix} 1 \\ \tan(\alpha/2) \end{bmatrix}, \quad r_{20} := \begin{bmatrix} \cos \alpha \\ \sin \alpha \end{bmatrix}.$$

The bi-21 map  $\rho_2$  has a sibling  $\sigma_2$  of total degree 2 defined by the template

$$r_{0,0,2} := r_{00}, r_{1,0,1} := r_{10}, r_{2,0,0} := r_{20}, r_{0,1,1} := \frac{r_{00}}{2}, r_{1,1,0} := \frac{r_{20}}{2}, r_{0,2,0} := \begin{bmatrix} 0 \\ 0 \end{bmatrix}.$$

Analogously,  $\rho$  has a sibling  $\sigma$  of total degree 3 defined by the cubic curve of  $\rho$  and the origin.

**3'.** We introduce the operator  $H^{55}$  that samples  $2 \times 2$  jets  $\partial_u^i \partial_v^j \mathbf{x}$ ,  $i, j \in \{0, 1, 2\}$  at the corners of the polynomial pieces to construct tensor-borders (of degree 5).

**$C^2$  capping of total degree 9** To cap without a collapsed edge, we here choose the central pieces to be ‘triangular’, i.e. of total degree  $d$  (which could in turn be represented by three quad patches of degree  $bi-d$ ).

#### Algorithm II: $C^2$ cap construction of total degree 9

*Input* The  $C^2$  cap  $\mathbf{x}$  of degree 6-5 constructed by Algorithm I and the tensor-border  $\mathbf{b} := J(\mathbf{x}, 1)$  ( $\mathbf{b} := J(\mathbf{x}, \frac{1}{2})$  for double bisection; see \* below).

*Output* A  $C^2$  cap consisting of  $N := 3n$  patches of total degree 9; plus  $N$  patches of degree  $bi-95$  for one bisection (plus  $n$  patches of degree 6-5 for double bisection).

*Algorithm.* (i) Bisect  $\mathbf{x}$  radially once or twice (see Figure 8).

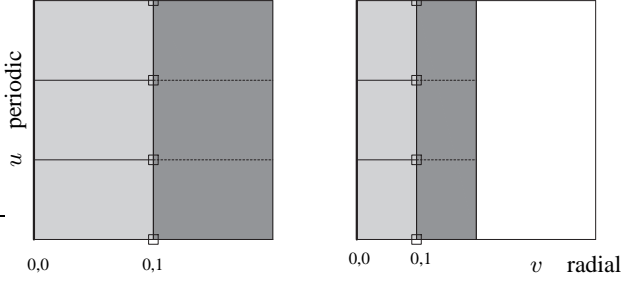


**Fig. 8. Radial bisections** followed by tri-section at the pole. (*left*) Once, (*right*) twice. In both cases, we associate  $v = 0$  with the collapsed edge of  $\mathbf{x}$  and  $v = 1$  at the boundary between the gray regions of the domain. The light grey region is the focus of Algorithms II, III, IV.

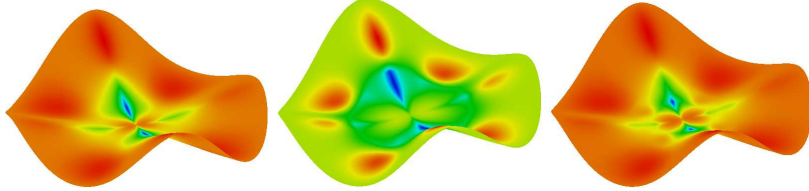


**Fig. 9. Single vs double split.** (*left*) Gauss curvature shading of a 6-5 cap (input Figure 2 *middle left*); (*middle*) Gauss shading of degree 9 construction corresponding to one bisection; (*right*) Gauss shading of degree 9 construction corresponding to the double split in Figure 8 *right*.

\* For elliptic configurations such as in Figure 1 *left*, the single bisection displayed in Figure 8 *left* suffices. For higher-order saddles, we recommend the double split of Figure 8 *right*, resulting in Figure 9 *right*.

Then tri-sect the subpatches at the pole and in the layer next to it so that the new polar valence is  $N$ . Apply  $H^{55}$  at the locations marked by  $\square$  in Figure 8 to generate a tensor-border of degree 5 in B-spline form.

(ii) Compose  $\mathbf{c} \circ \rho$  to yield a map of degree bi-93 with  $6 + N$  undetermined coefficients of  $\mathbf{c}$ . Apply  $H^{55}$  at the same locations as in (i) to form a second tensor-border of degree 5 in B-spline form.

(iii) Set the central point of  $\mathbf{c}$  to the central point of the 6-5 cap  $\mathbf{x}$ . Determine the remaining  $N + 5$  coefficients of  $\mathbf{c}$  by minimizing the sum of squared distances between the B-spline control points generated in (i) and (ii).

(iv) The inner cap corresponding to  $v \in [0..1]$  is defined by  $\mathbf{c} \circ \sigma$ , in essence trimming  $\mathbf{c}$  along the degree 3 boundary of  $\rho$ . Since we trisected, this yields three patches of total degree 9 per sector.

(v) For radial parameter  $v \in [1..2]$  the surrounding surface ring consists of  $N$  patches of degree bi-95 defined by

$$H_{N,9}(J(\mathbf{c} \circ \rho, 1); \mathbf{b}),$$

i.e. the tensor-border of  $\mathbf{c} \circ \rho$  at  $v = 1$  (consisting of  $N = 3n$  pieces) and the tri-sected and degree-raised tensor-border.

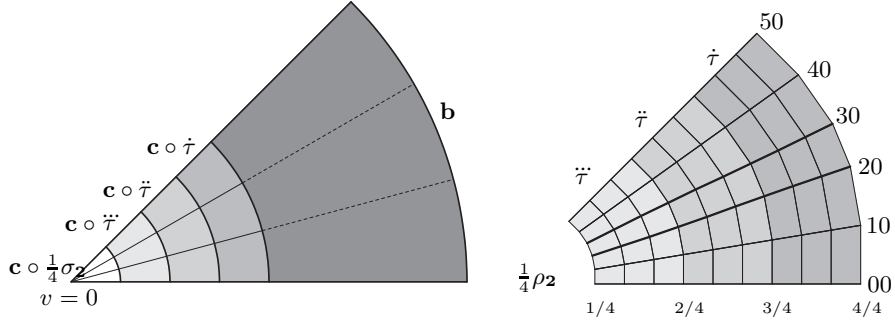


**Fig. 10.**  $G^2$  capping with a  $5 \times 3$ -split. (left) One sector is covered by 15 patches. (right) One sector of the domain transition map  $\tau$  of degree bi-53 (corresponding to the middle three surface rings of one sector after tri-section in the circular direction left, i.e. valence  $N = 3n$ ;  $\tau$  is symmetric with respect to the bisectrix of the sector. The radial curves starting inward at 00 and 10 and symmetrically at 40, 50 are straight lines. Only the two heavy-set lines starting at 20 and 30 are truly of piecewise degree 3.

**$G^2$  capping of total degree 6** Here we use a map  $\tau : [0..1]^2 \rightarrow \mathbb{R}^2$  (Figure 10 right) to transition from  $C^2$  to  $G^2$  constraints. It consists of three  $C^2$ -connected pieces  $\dot{\tau}, \ddot{\tau}, \ddot{\tau}$  of piecewise degree bi-53. Since the radial degree of each piece is 3,  $J(\tau, \frac{1}{4}) := J(\frac{1}{4}\rho_2, 1)$  (the  $C^2$  prolongation of  $\frac{1}{4}\rho_2$ ) and  $J(\tau, 1)$ , defined by rotations of the sector template

$$\dot{\tau}_{00} := (1, 0), \quad \dot{\tau}_{10} := \left(1, \frac{2}{5} \tan \frac{\alpha}{2}\right), \quad \dot{\tau}_{20} := \left(\frac{1}{10}(9 + \cos \alpha), \frac{4}{5} \tan \frac{\alpha}{2}\right); \quad (4)$$

$$\dot{\tau}_{\ell 1} := \frac{11}{12} \dot{\tau}_{\ell 0}, \quad \dot{\tau}_{\ell 2} := \frac{5}{6} \dot{\tau}_{\ell 0}, \quad \ell = 0, 1, 2, \quad (5)$$

determine  $\tau$  on  $[0..1] \times [\frac{1}{4}..1]$  as a  $C^2$ -connected map in radial direction whose outermost tensor-border is  $C^2$  in the periodic direction.

### Algorithm III: $G^2$ cap construction of total degree 6

**Input:** The tensor-border  $b$  and the cubic  $C^2$  cap  $c$  constructed by Algorithm II; the  $G^2$  polar parameterizations  $\rho_2$  and  $\sigma_2$ .

**Output:**  $N := 3n$  triangular patches of total degree 6, plus  $2N$  patches of degree 6-5 corresponding to  $v = [\frac{1}{4}.. \frac{1}{2}]$  and a surrounding ring (darkest gray in Figure 10) plus  $2N$  patches of degree bi-5 corresponding to  $v = [\frac{1}{2}..1]$ .

**Algorithm:** (a) Compose  $c \circ \frac{1}{4}\sigma_2$  to obtain the inner cap, corresponding to  $v \in [0.. \frac{1}{4}]$ , of  $N$  triangular Bézier patches of degree 6 (see Figure 10 left).

(b) Apply  $H^{55}$  to the composition  $c \circ \tau$  to form three intermediate bi-5 rings corresponding to  $v = [\frac{1}{4}..1]$ . The  $N$  patches corresponding to  $v = [\frac{1}{4}.. \frac{1}{2}]$  are made to match  $J(c \circ \frac{1}{4}\rho)$  and thereby to join with curvature continuity the inner cap constructed in (a). (c) The outermost  $N$  patches are constructed as in Algorithm II to meet the outer tensor-border of the patches constructed in (b) in a parametrically  $C^2$  fashion.

Since the degree of  $\partial_u^j(\tau)$  at  $u = 0$  is 1,1,3 for  $j = 0, 1, 2$  (and symmetrically at  $u = 1$ , the other sector boundary) the degree of  $\partial_u^j(c \circ \tau)$  at  $u = 0$  is 3,3,5 for  $j = 0, 1, 2$ .

So we can apply  $H^{55}$  to obtain a surface ring of degree bi-5 that reproduces this second order expansion at both sector boundaries. At  $v = \frac{1}{4}$ , the  $2 \times 2$  jets also coincide with that of  $c \circ \frac{1}{4}\rho_2$ . Therefore the construction in (b) ensures curvature continuity across  $v = \frac{1}{4}$  and this completes the proof of curvature continuity of the overall construction.

The number of patches is high ( $15n$  if one bisection is applied,  $16n$  if we radially bisect twice as in Figure 8 *right*). Figure 11 justifies trisection in the periodic direction, echoing the theme that polar layout prefers high valencies.

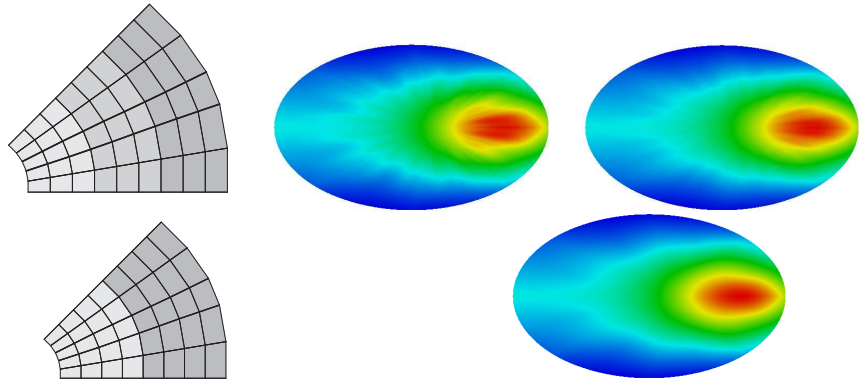


**Fig. 11. Bi-6  $G^2$  construction** of Algorithm III applied to the net of Figure 2. (top) (left) three rings of one third of a sector of  $\tau$ . (middle and right) Gauss curvature of the surface is shown for three rings and a tensor-border split into (top, middle) two subsectors, (top, right) three subsectors. (bottom) Construction with two subsectors and two rings of degree bi-6.

Instead of trisecting in the periodic direction, we can improve the shape by bisecting, replacing the three rings of degree 5-3 in  $\tau$  by two rings of degree 5-4 and applying the operator  $H^{66}$  of [5] to obtain bi-6 patches. Figure 11 *bottom*, shows the reparameterization patchwork, reduced to  $2 \times 2n$  patches instead of  $3 \times 3n$  resulting in a better curvature distribution.

### 3.2 $G^2$ capping of degree bi-5

A slight modification of Algorithm III yields a curvature continuous cap of degree bi-5 with one collapsed edge. This does not contradict Theorem 2 since the transitions between sectors are  $G^2$ , not parametrically  $C^2$ . Note that Algorithm IV accepts as input a tensor-border of at most degree 5.

#### Algorithm IV: $G^2$ cap construction of degree bi-5.

*Input:* The tensor-border  $b$  and the cubic  $C^2$  cap  $c$  constructed by Algorithm II; the  $G^2$  polar parameterization  $\rho_2$ .

*Output:*  $5N := 15n$  patches of degree bi-5 with the  $N$  innermost having one edge collapsed.

*Algorithm:* (a) Apply  $H^{55}$  to  $\mathbf{c} \circ \frac{1}{4}\rho_2$  to yield an innermost bi-5 cap with collapsed edge.  
 (b) and (c) mimic those of Algorithm III.

Since the degree of  $\partial_u^j \rho_2$ , for  $j = 0, 1, 2$  at  $u = 0$  and  $u = 1$  is 1,1,2, the operator  $H^{55}$  applied to  $\mathbf{c} \circ \frac{1}{4}\rho_2$  reproduces the second order expansion at both sector boundaries. Therefore the innermost bi-5 patches with collapsing edges form a  $G^2$  connected cap except possibly at the pole. Since the expansion at the pole is determined by  $\partial_v^j(\mathbf{q} \circ \frac{1}{4}\rho_2)$ ,  $j = 0, 1, 2$ , we can retrace the proof of curvature continuity at the pole from Theorem 1. Figure 12 shows the bi-5 patchwork corresponding to Figure 2.

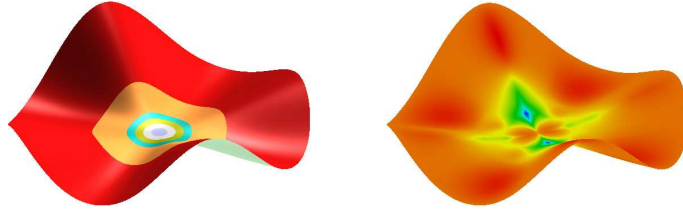


**Fig. 12. Bi-5 construction.** (left) Rings of the cap surface; (right) its Gauss curvature shading.

## 4 Extensions and Discussion

The main construction, Algorithm I, generates a 6-5 cap appropriate for most geometry processing pipelines. Due to the resulting good shape, the caps were used as a guide surface in the subsequent sections. Algorithms III and IV generate many  $(15n)$  patches mainly to obtain a fair transition from  $G^2$  connections at the central point to the  $C^2$  input.

If the tensor-border is appropriately  $G^2$ , we can use  $\rho_2$  to replace the 6-5 cap of Algorithm I by an outer ring of patches of degree bi-4 and an inner cap of degree bi-4 with edges collapsed to the central point. A  $C^2$  bi-3 polar subdivision can be obtained by converting the 6-5 patch to the accelerated bi-3 form of [13]. (We need only apply de Casteljeau's algorithm repeatedly in the periodic direction to obtain the required  $2 \times 2$  jets in bi-3 form.)

Alternatively, sampling the corner jets of the 6-5 patches results in high quality cappings that are  $C^1$  at the pole and  $C^2$  away from it. We can generate such surfaces of bidegree bi-5 with one patch per sector, bi-4 with four patches per sector, or bi-3 with nine patches per sector, trading degree for number of pieces. As with the curvature bounded subdivision algorithms in [14] and the constructions displayed in Figure 11, the lower the degree, the more the curvature fluctuates.

An important bonus of the polar layout, illustrated in Figure 13, is that we can adjust the  $C^2$  bi-31 ct-map  $\rho$  to non-uniform spacing, simply by manipulating its cubic spline boundary.

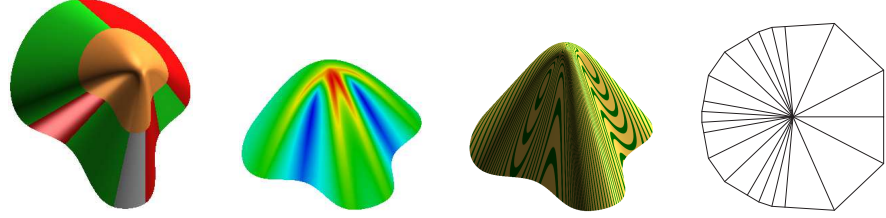


**Fig. 13.** (left) Highly non-uniform input from conical surfaces capped by Algorithm I with non-uniform ct-map. (middle left) Gauss curvature shading of capping; (middle right) highlights. (right) The non-uniform bi-31 ct-map.

## References

1. Myles, A., Karčiauskas, K., Peters, J.: Extending Catmull-Clark subdivision and PCCM with polar structures. In: PG '07: Proceedings of the 15th Pacific Conference on Computer Graphics and Applications, Washington, DC, USA, IEEE Computer Society (2007) 313–320
2. Karčiauskas, K., Peters, J.: Bicubic polar subdivision. ACM Trans. Graph. **26**(4) (2007) 14
3. Prautzsch, H., Boehm, W., Paluszny, M.: Bézier and B-Spline Techniques. Springer Verlag (2002)
4. Catmull, E., Clark, J.: Recursively generated B-spline surfaces on arbitrary topological meshes. Computer Aided Design **10** (1978) 350–355
5. Karčiauskas, K., Peters, J.: Concentric tesselation maps and curvature continuous guided surfaces. Computer-Aided Geometric Design **24**(2) (Feb 2007) 99–111
6. Prautzsch, H.: Freeform splines. Computer Aided Geometric Design **14**(3) (1997) 201–206
7. Reif, U.: TURBS—topologically unrestricted rational  $B$ -splines. Constructive Approximation. An International Journal for Approximations and Expansions **14**(1) (1998) 57–77
8. Loop, C.: Second order smoothness over extraordinary vertices. In: Symposium on Geometry Processing. (2004) 169–178
9. Karčiauskas, K., Peters, J.: Guided spline surfaces. Computer Aided Geometric Design (2009 N1) 1–20
10. Loop, C.T., Schaefer, S.:  $G^2$  tensor product splines over extraordinary vertices. Computer Graphics Forum (Proceedings of 2008 Symposium on Geometr++y Processing) **27**(5) (2008) 1373–1382
11. Bohl, H., Reif, U.: Degenerate Bézier patches with continuous curvature. Computer Aided Geometric Design **14**(8) (1997) 749–761
12. Peters, J., Reif, U.: Subdivision Surfaces. Volume 3 of Geometry and Computing. Springer-Verlag, New York (2008)
13. Karčiauskas, K., Peters, J.: Guided subdivision. Technical Report 2008-464, Dept CISE, University of Florida (2008) posted since 2005 at <http://www.cise.ufl.edu/research/SurfLab/papers.shtml>.
14. Karčiauskas, K., Peters, J.: On the curvature of guided surfaces. Computer Aided Geometric Design **25**(2) (feb 2008) 69–79